Hindawi
Shock and Vibration
Volume 2019, Article ID 4281514, 11 pages
https://doi.org/10.1155/2019/4281514

Research Article

Estimation of Cement Asphalt Mortar Disengagement Degree Using Vehicle Dynamic Response

Hui Shi[1,2], **Liqiang Zhu**[1,2], **Hongmei Shi**[1,2] **and Zujun Yu**[1,2]

[1]*School of Mechanical, Electronic and Control Engineering, Beijing Jiaotong University, Beijing 100044, China*
[2]*Key Laboratory of Vehicle Advanced Manufacturing, Measuring and Control Technology (Beijing Jiaotong University), Ministry of Education, Beijing 100044, China*

Correspondence should be addressed to Hongmei Shi; hmshi@bjtu.edu.cn

Received 4 October 2018; Revised 6 December 2018; Accepted 19 December 2018; Published 3 January 2019

Guest Editor: Alessandro Sabato

Cement asphalt mortar (CA) disengagement of a ballastless track will induce changes of dynamic response of a passing vehicle, which can accordingly be used to estimate the disengagement degree. In this paper, a novel method called CA mortar disengagement degree estimation algorithm (CMDEA) is proposed through an analysis of wheel acceleration of a passing vehicle. The disengagement degree estimation is transformed into an optimization problem by regarding the CA mortar disengagement degree as a parameter of a vehicle-track coupling model. An improved genetic algorithm with a shifting window is employed for the parameter optimization, which is split into a number of phases and whose initial values are given in terms of a priori probabilities. The accuracy and robustness of the estimation are discussed, and the results are compared with regular genetic algorithm. The simulation results show that CMDEA can estimate CA mortar degrees with an acceptable accuracy. Meanwhile, the proposed algorithm has the advantages of a lower error value and much shorter computation time. Moreover, the robustness of the algorithm under different vehicle speeds, track irregularities, and signal noise levels is also verified.

1. Introduction

With the commissioning of the Beijing-Tianjin intercity railway in 2008, the running mileage of China's high-speed railways has exceeded 20,000 kilometers. As high-speed railways are being rapidly developed, ballastless track has been widely adopted in many countries due to its advantages of good stability, good durability, and less maintenance [1]. The understructure of the China Railway Track System II-type (CRTSII) slab ballastless track consists of track slabs, a cement-emulsified asphalt (CA) mortar layer, a support layer, and an embankment. As the speed of vehicles increases greatly, the dynamic effects between wheels and rails also increase, resulting in the strengthening of the dynamic effect on infrastructure. As CA mortar is a key component of the elastic adjustment layer in ballastless track, its performance directly affects the service durability of slab ballastless track equipment. Due to the difficulty of construction quality control and the warping effect of track slabs, CA mortar will often deteriorate to varying degrees. When the entire CA mortar layer is separated from the interface of the track slab, it will give rise to a complete loss of cohesion, a phenomenon known as CA mortar disengagement. If it is not repaired in time, it will accelerate the structural damage of track and even have adverse effects on traffic safety. Therefore, CA mortar disengagement detection is necessary to ensure the safety of vehicle operations and formulate a timely rail line maintenance plan.

Presently, extensive research on nondestructive testing has been carried out in the field of concrete defect detection. Nevertheless, the references on CA mortar disengagement identification are countable, most of which is focused on the impulse hammer excitation method. Chen [2] evaluated the effectiveness of elastic wave detection in the underline

layered structure based on elastic wave propagation theory in layered media and the time frequency characteristics of elastic wave fields. Hu [3] researched the propagation velocity and laws of stress waves in track slabs and estimated the depth of honeycombing using the impact-echo method. Zhong et al. [4] proposed a detection method based on a detector array group for elastic wave propagation in multilayer media, which can effectively detect the spatial distribution of segregations among CA mortar layers. Tian et al. [5] discussed the feasibility of mortar defect detection using the transient elastic wave method. The results showed that the defects of CA mortar can be detected using the characteristics of frequency band peaks and the power density values of elastic waves. Li et al. [6] applied gradient boosted regression trees (GBRT) to CA mortar disengagement detection using a sound signal produced by a passing train to detect the damage qualitatively. The aforementioned methods based on the impulse hammer can only be carried out in the period of skylight time with the shortcomings of low efficiency and limited identification area.

Service condition monitoring of railway infrastructures using passing vehicles has been a new research area since 2000 and shows promising results in structural health monitoring [7]. Its main premise is that differences in the physical properties of track structure such as mass, stiffness, and damping will give rise to changes in vibration characteristics. A direct detection method is to install sensors on the track and detect damages by analysing the vibration responses of the track. This requires a large number of sensors to be laid along the track. An alternative, more cost-efficient detection method is to mount sensors on vehicles and detect track damages utilizing the dynamic responses of the vehicles. The last two decades have seen a rise in studies attempting to detect bridge damage using indirect vibration-based methods. Yang et al. [8, 9] firstly proposed the theory of extracting the first-order natural frequency of bridges from vehicle response and then carried validation tests. Zhang et al. [10] described a new method based on operating deflection shape curvature extracted from the dynamic response of a passing vehicle, which can be used to detect local damages in beam and plate-like structures. Molodova et al. [11] employed a model to determine a quantitative relationship between the characteristics of the axle box accelerations and short track defects. On-board methods using vehicle dynamic responses have the potential to be used as a monitoring tool to estimate track infrastructure conditions. Nonetheless, most of these indirect methods utilize low-speed vehicles and involve disturbing normal rail traffic.

In recent years, more and more researchers have introduced intelligent sensing algorithms into vehicle-based indirect methods. Li and Au [12] suggested a multistage damage detection method based on modal strain energy and a genetic algorithm to determine the location of damage in a two-span continuous bridge. Quirke et al. [13] proposed a method to estimate railway track stiffness using a cross-entropy optimization technique. Li et al. [14] employed a method based on the generalized pattern search algorithm to identify bridge parameters indirectly using a passing vehicle.

Typical intelligent optimization algorithms include simulated annealing (SA), the gradient descent method, genetic algorithm (GA), etc. Although simulated annealing and gradient descent method achieve fast convergence in local optimizations, they can easily fall into local minima, resulting in a weak global search ability, low optimization performance, and slow or even no global convergence. Moreover, the gradient descent method involves computing the derivatives, which can be hard for large nonlinear problems. Genetic algorithm, first proposed by John Holland in 1975, achieves the adaptability of individuals through the mechanics of natural selection, crossover, and mutation by means of biogenetics and simulates the evolution process of nature. It is a nonderivative-optimized stochastic optimization search algorithm with strong global search ability and robustness. As an adaptive global probability search algorithm, GA is very suitable for solving complex nonlinear optimization problems. Therefore, it is widely used in global optimization [15, 16], search [17], and machine learning [18] contexts. In order to overcome the shortcoming of long running time of regular genetic algorithm, an improved genetic algorithm is employed in this paper, which is split into a number of phases and whose initial values are given in terms of a priori probabilities.

At present, the research on the estimation of CA mortar disengagement degree based on dynamic responses of passing vehicles is still a blank field. A novel method is proposed in this paper for the estimation of CA mortar disengagement degree through an analysis of vehicle wheel accelerations. The method is referred to throughout the paper as the CA mortar disengagement degree estimation algorithm (CMDEA). The vehicle-track coupling model with the CA mortar disengagement model used in this paper and the simulation result of dynamic response are described in Section 2. The CA mortar disengagement degree estimation algorithm is introduced in Section 3. Numerical simulation results are demonstrated and analysed in Section 4, and the robustness of the proposed algorithm under different conditions is validated in Section 5.

2. Model Description

2.1. Vehicle Model. As shown in Figure 1(a), the vehicle is modelled as a multirigid system that moves on a track structure at the speed of v and consists of three masses: m_c representing the car body mass, m_t representing the bogie mass, and m_w representing the wheel mass [19]. In consideration of the vertical translation and nodding motion of the car body and the bogies, and the vertical translation of the wheels, the vehicle system has 10 degrees of freedom (DOFs). The components are connected by elastic springs and dampers, representing the secondary and primary suspension of the vehicle, respectively.

The general form of the equation of motion for the vehicle system can be represented as follows:

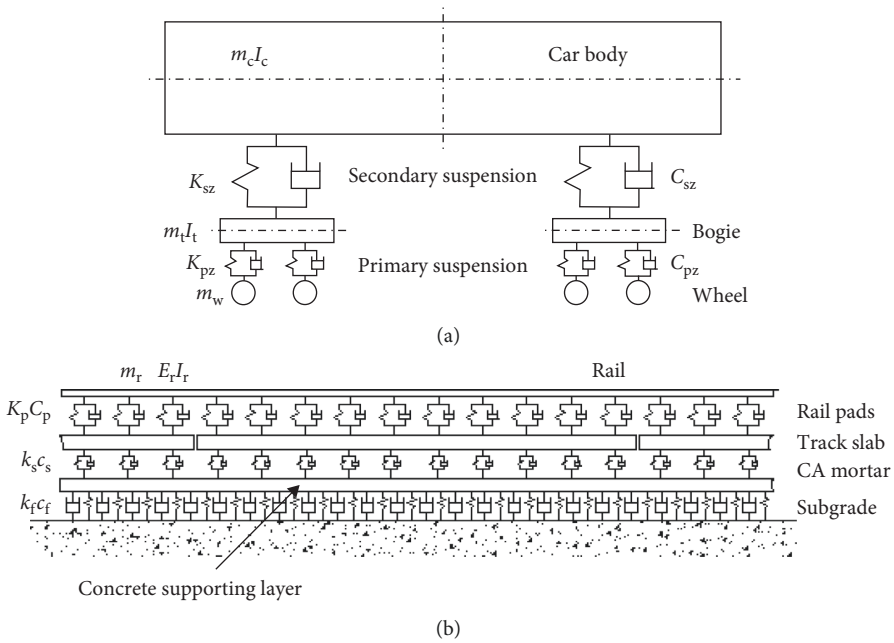

Figure 1: Vehicle and track model: (a) vehicle model; (b) ballastless slab track model.

$$\mathbf{M}_v\ddot{\mathbf{x}}_v + \mathbf{C}_v\dot{\mathbf{x}}_v + \mathbf{K}_v\mathbf{x}_v = \mathbf{p}_v, \quad (1)$$

where $\mathbf{M}_v$, $\mathbf{C}_v$, and $\mathbf{K}_v$ are the mass, damping, and stiffness matrices of the vehicle; the vectors $\mathbf{x}_v$, $\dot{\mathbf{x}}_v$, and $\ddot{\mathbf{x}}_v$ are the vehicle displacements, velocities, and accelerations, respectively; and $\mathbf{p}_v$ is the force vector of the vehicle system.

2.2. Track Model. As shown in Figure 1(b), the track system is modelled here as a beam continuously supported on a triple-layer spring-damper system, which represents the rail pads, CA mortars, and subgrade, respectively.

The general form of the equation of motion for the track system can be represented as follows:

$$\mathbf{M}_t\ddot{\mathbf{x}}_t + \mathbf{C}_t\dot{\mathbf{x}}_t + \mathbf{K}_t\mathbf{x}_t = \mathbf{p}_t, \quad (2)$$

where $\mathbf{M}_t$, $\mathbf{C}_t$, and $\mathbf{K}_t$ are the global mass, damping, and stiffness matrices of the track system; the vectors $\mathbf{x}_t$, $\dot{\mathbf{x}}_t$, and $\ddot{\mathbf{x}}_t$ are the track system displacements, velocities, and accelerations, respectively; and $\mathbf{p}_t$ is the force vector of the track system.

The China Railways High-speed 2 (CRH2) electric multiple unit (EMU) trailer and the high-speed line with China Railway Track System II-type (CRTS II) track slab are considered in this paper. The corresponding property values were gathered from the literature [19] and are listed in Tables 1 and 2.

2.3. Coupling Model. To determine the wheel-rail vertical force, we applied Hertz nonlinear elastic contact theory for the vehicle-track vertical coupling relationship. When the wheel tread is wear type, the expression of the wheel-rail vertical force is

Table 1: Properties for CRH2 EMU trailer.

Property	Unit	Symbol	Value
Mass of car body	kg	m_c	26100
Mass of bogie	kg	m_t	2600
Mass of wheel	kg	m_w	2100
Pitch moment of inertia of car	kg·m^2	I_c	1.28×10^6
Pitch moment of inertia of bogie	kg·m^2	I_t	1424
Stiffness of primary suspension	N/m	K_{pz}	1.176×10^6
Stiffness of secondary suspension	N/m	C_{pz}	9.91×10^5
Damping of primary suspension	N·s/m	K_{sz}	1.02×10^6
Damping of secondary suspension	N·s/m	C_{sz}	1.96×10^5
Half of rigid wheelbase	m	l_t	1.25
Half of length between the bogie pivot centers	m	l_c	8.75
Radius of wheel	m	R	0.43

Table 2: Properties for high-speed line.

Property	Unit	Symbol	Value
Elastic modulus of rail	N/m^2	E_r	2.059×10^{11}
Rotational inertia of rail	m^4	I_r	3.217×10^{-5}
Mass of rail per unit length	kg/m	m_r	60.64
Stiffness of rail pad	N/m	K_p	6×10^7
Damping of rail pad	N·s/m	C_p	7.5×10^4
Length between fasteners	m	L_p	0.65
Length of track slab	m	L_s	6.5 m
Mass of track slab	kg	m_s	8.3×10^3
Elastic modulus of track slab	MPa	E_s	3.9×10^4
Rotational inertia of track slab	m^4	I_s	3.32×10^7
Stiffness of CA mortar	N/m^2	k_s	1.25×10^9
Damping of CA mortar	N·s/m^2	c_s	3.458×10^4

$$p_j(t) = \begin{cases} \left\{\frac{1}{G}\left[x_{wj}(t) - x_r\left(x_{wj}, t\right) - x_0(t)\right]\right\}^{3/2}, & \left(x_{wj}(t) - x_r\left(x_{wj}, t\right) - x_0(t) > 0\right), \\ 0, & \left(x_{wj}(t) - x_r\left(x_{wj}, t\right) - x_0(t) < 0\right), \end{cases} \tag{3}$$

where $j = 1 \sim 4$; $x_{wj}(t)$ and $x_r(x_{wj}, t)$ represent the vertical displacement of the jth wheel and the rail at the jth wheel-rail contact position at time t, respectively; $x_0(t)$ represents the track irregularity at the wheel-rail interface; and G is the Hertzian contact coefficient.

The expression of the force vector of the vehicle system is

$$\mathbf{p}_v = \{m_c g \;\; 0 \;\; m_t g \;\; 0 \;\; m_t g \;\; 0 \;\; m_w g - 2p_1(t) \;\; m_w g - 2p_2(t) \;\; m_w g - 2p_3(t) \;\; m_w g - 2p_4(t)\}^T. \tag{4}$$

The expression of the force vector of the track system is

$$\mathbf{p}_t = \left[\sum_{j=1}^{4} p_j(t) Y_k\left(x_{wj}\right), \mathbf{0}_{1\times(m\times NMS)}, \mathbf{0}_{1\times NMSS}\right]^T, \quad (k = 1 \sim NM), \tag{5}$$

where NM, NMS, and NMSS are the modal orders of the rail, track slab, and concrete supporting layer, respectively, and m is the number of track slabs in the model. Y_k is the modal shape function of rail, the expression of which can be written as follows:

$$Y_k(x) = \sqrt{\frac{2}{m_r L}} \sin \frac{k\pi x}{L}. \tag{6}$$

2.4. Track Irregularity. Considering the influence of track irregularity on the vibration of the coupling model, a time domain random irregularity sample is generated using the China ballastless track power spectral density (PSD) function $S(f)$ proposed by the China Academy of Railway Sciences. The fitting equation is as follows:

$$S(f) = mf^{-k}, \tag{7}$$

where the unit of $S(f)$ is $mm^2/(1/m)$; f is the spatial frequency (1/m); m and k are fitting coefficients. The time domain random irregularity sample of the China ballastless track spectrum is calculated using the inverse fast Fourier transform (IFFT) method.

2.5. CA Mortar Disengagement Model. The condition of CA mortar disengagement can be simulated as a loss in stiffness by changing the coefficients of the elastic spring and damper that represent CA mortar in the corresponding areas [20]. In order to simulate the disengagement, a discrete CA mortar model is established, in which a CA mortar is divided into many units of longitudinal length l_s [21].

The CA mortar disengagement model is shown in Figure 2. The direction along the rail is the longitudinal direction, while the direction which is vertical to the rail is the lateral direction. The CA mortar disengagement condition can be measured by two parameters, one of which is the CA mortar longitudinal disengagement length l and the other is the lateral disengagement degree of the ith CA mortar unit d_i.

As illustrated in Figure 2, d_i can be expressed as

$$d_i = 1 - \frac{b_i}{b_0}, \tag{8}$$

where b_0 is the overall track slab width (2.55 m for CRTS II track slab), and b_i is the width of the ith CA mortar unit where no disengagement has occurred. Hence, $d_i = 1$ indicates that the ith CA mortar unit is completely disengaged in the lateral direction, whereas $d_i = 0.7$ implies that 70% of the ith CA mortar unit in the lateral direction is disengaged. Then the supporting force of the ith CA mortar unit on the track slab can be expressed as

$$F_{sri} = d_i \cdot k_s \cdot \left(x_r - x_s\right) + d_i \cdot c_s \cdot \left(\dot{x}_r - \dot{x}_s\right), \tag{9}$$

where x_r and x_s are the displacement of the rail and the track slab, respectively.

When the CA mortar disengagement longitudinal length is less than 0.65 m, the effect of disengagement on the wheel acceleration is not obvious [22, 23]. Consequently, 0.65 m will be considered as longitudinal length of one unit in this model, i.e., $l_s = 0.65$ m. Therefore, the CA mortar longitudinal disengagement length l can be evaluated by unit, while the lateral disengagement degree d of each unit is the value we want to estimate and is the focus in this paper.

The schematic diagram of the overall model used in this paper is shown in Figure 3. The simulated length in this paper is 16 track plates, i.e., 104 m. The position of the track slab is represented by No. 1~No. 16. For the CRTS II ballastless track considered in this paper, there are 10 CA mortar units corresponding to a piece of track slab. Considering the length of track occupied by the vehicle (20 m for CRH2 EMU) and the boundary effect of wheel acceleration signal, the CA mortar disengagement condition of the first 5 and the last piece's track slab (No. 1~No. 5, No. 16) is assumed to be known. In this paper, we aim at estimating the disengagement degree parameters of the subsequent 10 pieces track slabs (No. 6~No. 15), regardless of the boundary effect, which corresponds to 100 units ($D = [d_1, d_2, \ldots, d_{100}]$). The subscript number i ($i = 1 \sim 100$) represents the order number of each CA mortar unit.

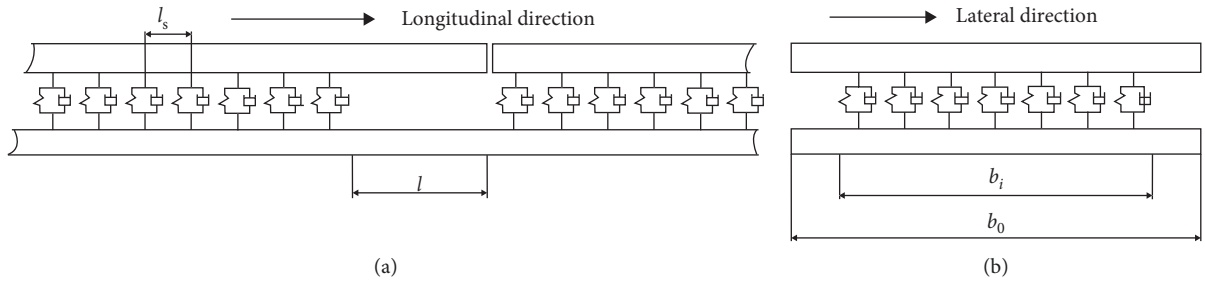

Figure 2: CA mortar disengagement model: (a) longitudinal view; (b) lateral view.

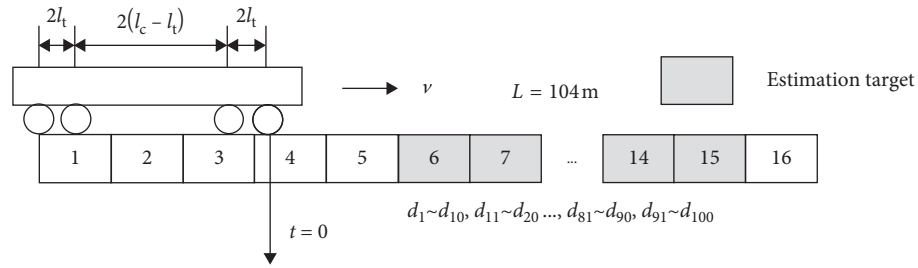

Figure 3: Schematic diagram of the overall model.

2.6. Simulation Results. To assess the concept of CMDEA in this paper, numerical simulations for the vehicle-track coupling model are used. A hypothetical CA mortar disengagement condition was used to demonstrate the capabilities of CMDEA. The values of the hypothetical condition of CA mortar disengagement referred to here as the "actual" values are as follows:

$$\begin{aligned} d_{11} &= 0.2, \\ d_{31} &= 0.4, \\ d_{51} &= 0.6, \\ d_{71} &= 0.8, \\ d_{91} &= 1, \end{aligned} \tag{10}$$

with the disengagement degrees of other units set to 0.

The equations of the coupling model are solved using the multistep prediction-correction based on Newmark's method, as developed by Zhai for Matlab [19]. A vehicle travels over a track at a constant speed of 300 km/h. The scanning frequency used for all simulations is 10 kHz. The simulated acceleration signal of the front wheel when a vehicle crosses a track model including the hypothetical CA mortar disengagement condition is taken as the "measured" signal, shown in Figure 4. Then, the simulated response ("measured" signal) is input into CMDEA, which was used to estimate the CA disengagement degrees.

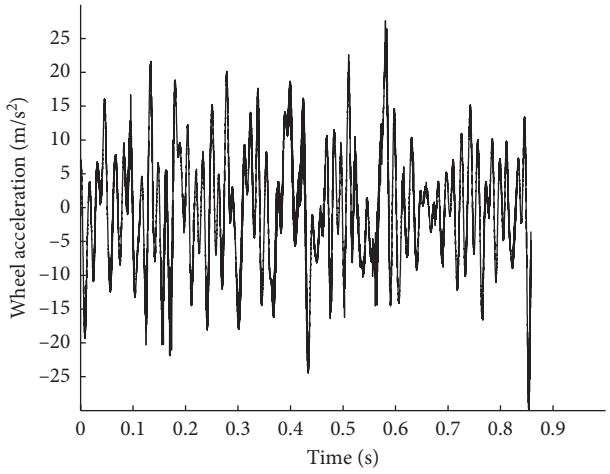

Figure 4: Simulated signal of wheel acceleration.

3. CA Mortar Disengagement Degree Estimation Algorithm (CMDEA)

A CA mortar disengagement degree estimation algorithm is described in this section based on an adapted genetic optimization algorithm. The disengagement degree estimation is transformed into an optimization problem by regarding the disengagement degree as a parameter of the vehicle-track coupling model.

3.1. CA Mortar Disengagement Degree Estimation Principle Using Genetic Algorithm. A genetic algorithm is applied in this paper to estimate CA mortar disengagement degrees from the dynamic responses of a passing vehicle as it crosses a track. Considering the CA mortar disengagement degrees as individuals, the parameters are transformed into a one-dimensional data string. The fitness of the individuals in each generation gradually increases utilizing the genetic operations and finally converges to a group of individuals that minimizes the objective function.

Firstly, a population of CA mortar disengagement degree vectors is generated randomly in the range of [0, 1]. For each seed in the population, a CA mortar disengagement degree

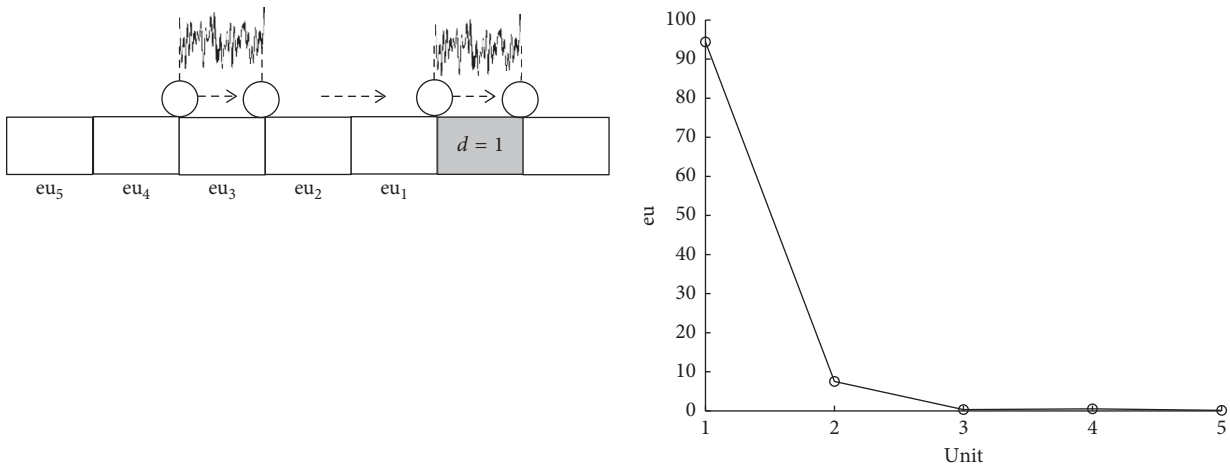

Figure 5: Boundary effects analysis: (a) diagram of effect index; (b) effect index ($l = 0.65$ m and $d = 1$).

matrix is produced, and the simulated acceleration signal of the wheel is calculated using the vehicle-track coupling model. An objective function value is then calculated to assess the quality of each seed.

In this paper, the objective function is taken as the sum of squared differences between the wheel accelerations calculated for each trial CA mortar disengagement degree matrix, $\widetilde{A}$, and the simulated wheel accelerations for the on-board measurement system, A'. The equation of the objective function is

$$O = \Delta E^2 = \sum_{i=1}^{n} \left(\widetilde{A} - A'\right)^2, \tag{11}$$

where n is the total number of scans in the acceleration signal.

3.2. Basis for the Structure of CMDEA. The disengagement of a CA mortar unit not only has an effect on the response of a vehicle when it passes the unit, but also has an effect when the vehicle passes the preceding units, as shown in Figure 5(a). In order to remove the boundary effects, it is necessary to include a number of units at the beginning of the estimation process. To quantify the effect of the disengagement unit on the wheel acceleration when a vehicle passes the preceding units, the effect index eu_i is defined as follows:

$$\mathrm{eu}_i = \sum_{j=1}^{n} \left(A_j - A_{0j}\right)^2, \tag{12}$$

where n is the number of sampling points in each unit; A_{0i} and A_i represent the wheel acceleration over healthy and damaged CA mortar, respectively; and the subscript number $i\,(i = 1, 2, 3, \ldots)$ represents the order number of the preceding unit.

Figure 5(b) shows the effect index of a CA mortar disengagement unit ($l = 0.65$ m and $d = 1$) on wheel acceleration when a vehicle passes the 5 preceding units. It can be seen that the effect index of the 1st unit is large, but diminishes as the distance from the disengagement unit becomes longer. The effect index of the 3rd unit is very small and can be ignored. Therefore, the effects of 2 preceding units need to be considered for the estimation process for each unit.

3.3. Improved Genetic Algorithm with a Shifting Window. The CA mortar disengagement degree varies along the track, which means the representing parameter d_i is different and multiple parameters need to be estimated. Considering the possibility of determining limit parameters for one optimization process, an adapted version of the genetic algorithm with a shifting window is used. The total estimation process is split into a number of phases, in which a smaller number of CA mortar disengagement degrees are estimated before proceeding to the next phase. Stepping through the CA mortar disengagement degrees in phases significantly reduces the dimensionality of the problem.

Due to the effects of varied CA mortar disengagement degrees on the dynamic response of a vehicle when it passes the 2 preceding units of a disengagement unit, a length of 4 units is used in CMDEA as a phase length. CA mortar disengagement degrees at each phase are estimated for the last 2 units of the phase. CMDEA steps through the CA mortar disengagement degrees in phases using the disengagement degree estimation template, as shown in Figure 6(a). Green represents known parameters; gray represents unknown parameters which will be estimated during the current phase; white represents unknown parameters which are set to 0. The CA mortar disengagement degree values for the first 2 units are obtained from the previous phase, whereas for the last 2 units, they are estimated in the current phase and are used as known values for the first 2 units in the next phase. In order to ensure the vehicle dynamic equilibrium at the start of each phase, initial values for the dynamic response vectors (displacement, velocity, and acceleration) of the coupling model in the

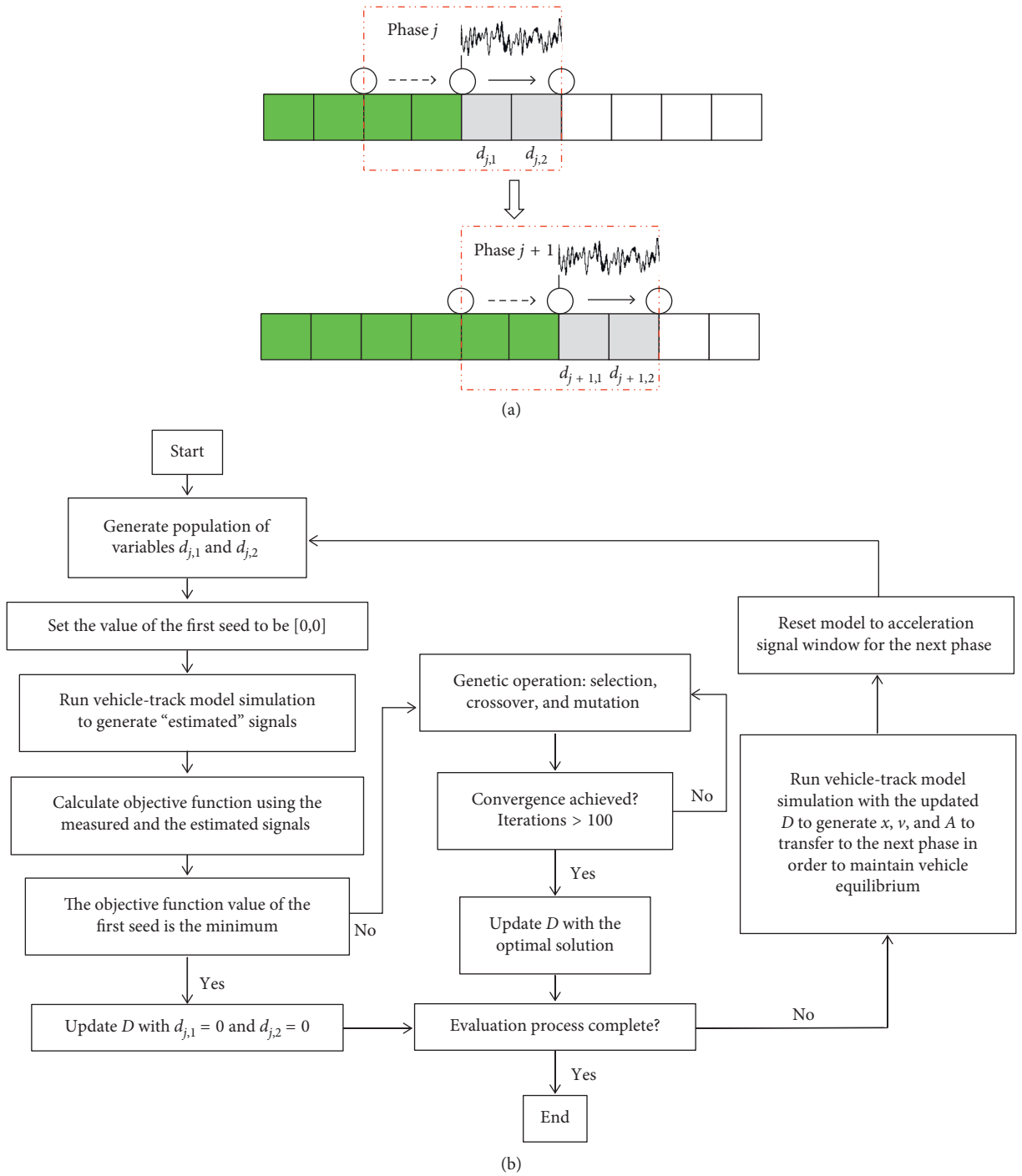

Figure 6: Improved genetic algorithm with a shifting window: (a) stepping procedure; (b) flowchart of CMDEA : Phase j.

current phase are transferred from the previous phase using the values estimated for the CA mortar disengagement degrees.

In view of the a priori probability that the CA mortar is healthy in most cases, i.e., $d_i = 0$, an improved genetic algorithm optimization process is employed in each phase. When the initial population is generated, the value of the first seed is initialized to [0, 0]. The sum of squares of the differences between the measured and the estimated signals is calculated. If the objective function value of the first seed is the minimum, the value of [0, 0] is then taken as the optimal solution in the current phase. Otherwise, the objective function values for all seeds in the population are ranked and genetic operations are carried out to improve the population of solutions in the next generation until convergence is achieved.

The process for estimating the CA mortar disengagement degrees in Phase j is shown in Figure 6(b).

4. Results and Discussion

The results of the numerical test of CMDEA for estimating the CA mortar disengagement are presented in this section. Parameters used in the CMDEA are listed in Table 3.

The objective function values of the optimal solution for the five damaged units at each iteration are illustrated in Figure 7(a). It is observed that the optimal solution of the function converges continuously during the evolution of the genetic algorithm, and the values of the objective function become smaller and smaller. It can be seen from the evolution process that at the beginning of the optimization, the seed optimization is rapid, and after 80 generations, the objective function value tends to stabilize. Therefore, 100 is taken as the upper limit of the number of iterations here.

The CA mortar disengagement degree estimation result is shown in Figure 7(b). The black circles represent the accrual values, whereas the red stars represent the estimated ones.

It can be seen from Figure 7(b) that the estimated values are almost consistent with the actual ones. In order to qualify the overall error between the actual and estimated values for CA mortar disengagement degrees, the margin of error E is defined as

$$E = \frac{\sqrt{\sum_{i=1}^{N}\left(d_i - \tilde{d}_i\right)^2}}{N}, \tag{13}$$

where i represents the order number of the unit, N represents the number of units to be estimated, and d_i and $\tilde{d}_i$ represent the actual and the estimated value of the ith unit, respectively.

Table 4 shows comparisons of error values and total computation time required for CMDEA using the regular genetic algorithm and the improved genetic algorithm, respectively. The simulations were performed using a 4 GHz processor and 16.0 GB of RAM running on Matlab.

Since the improved genetic algorithm simplifies the optimization processes for most healthy units and reduces the cumulative error, it has the advantages of a lower error value and much shorter total computation time compared with the regular genetic algorithm, as illustrated in Table 4. Therefore, the CMDEA used in this paper is effective for estimating CA mortar disengagement degrees with an acceptable accuracy.

5. CMDEA under Different Conditions

When vehicle speeds, track irregularities, and signal noise levels are different, the dynamic responses of the vehicle-track coupling system are also different. In order to verify the robustness of CMDEA, its performance under different conditions will be discussed in this section.

5.1. Influence of Vehicle Speeds. The dynamic response of a vehicle will change as the vehicle's speed changes. The wheel accelerations resulting from the vehicle-track model for speeds of 250 km/h and 360 km/h are investigated in this

Table 3: CMDEA parameters.

Property	Value
Population size	10
Maximum of iterations	100
Crossover probability	0.7
Mutation probability	0.25

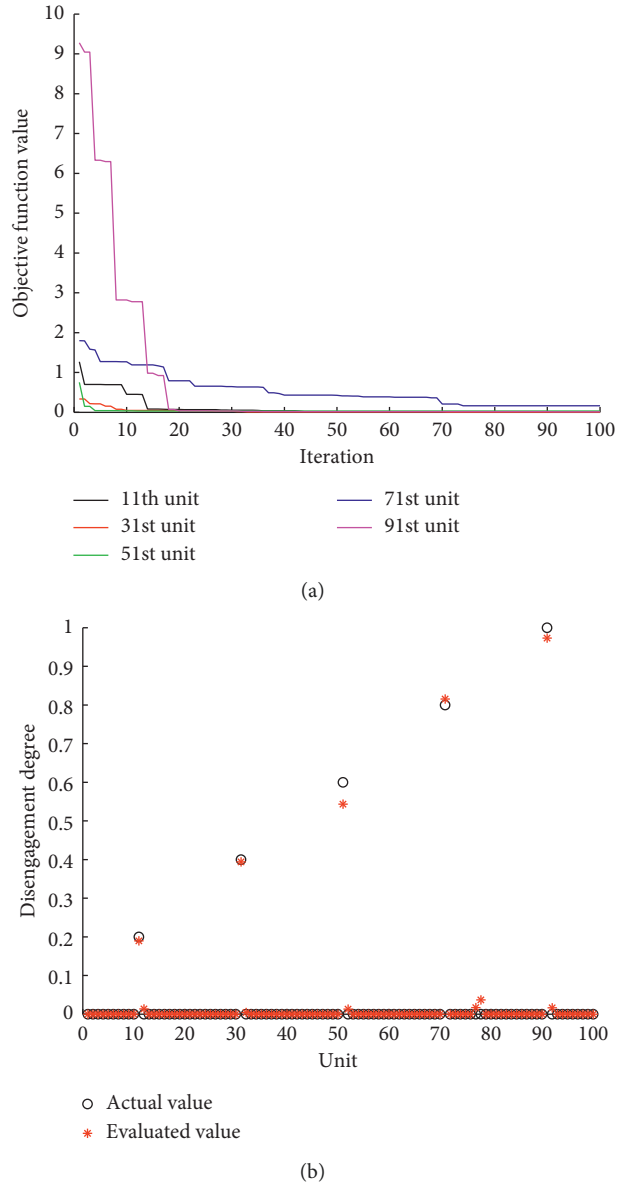

Figure 7: Simulation results: (a) objective function values for the optimal solutions at each iteration; (b) result of CA mortar disengagement degree estimation.

Table 4: Comparisons of error and computation time.

Algorithm	E	Computation time
Regular genetic algorithm	0.0021	150 h
Improved genetic algorithm	8.1020e-04	15 h

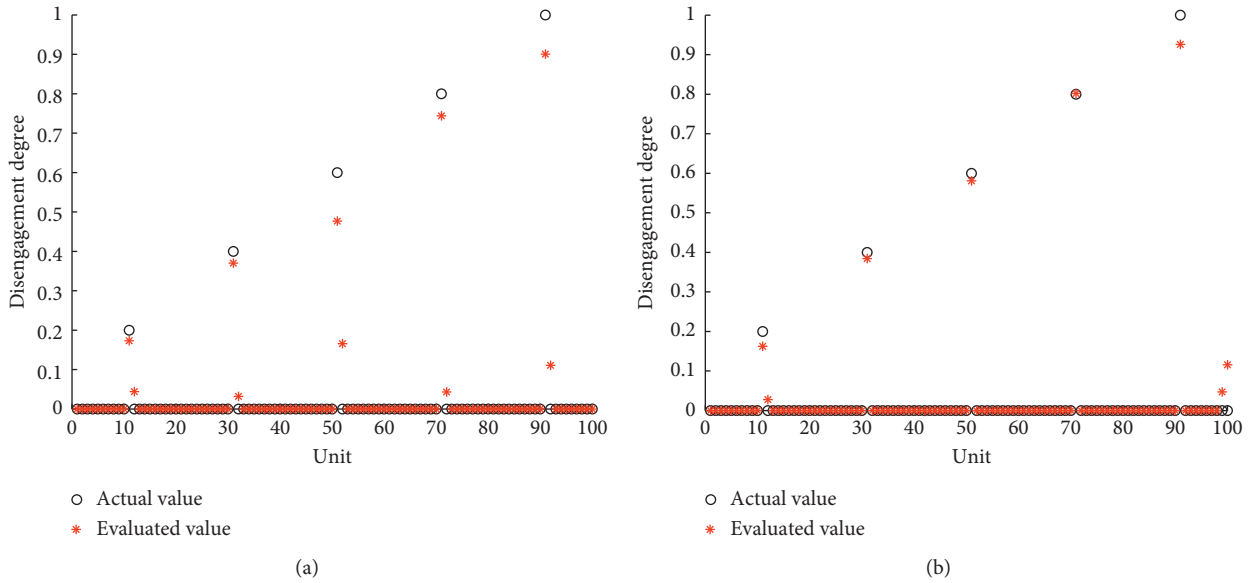

Figure 8: Estimation results of CMDEA under different vehicle speeds: (a) 250 km/h; (b) 360 km/h.

section. The other simulation parameters are the same as the above simulation. The estimation results under different vehicle speeds are shown in Figure 8.

According to equation (13), for vehicle speeds of 250 km/h and 360 km/h, the corresponding values of E are 0.0027 and 0.0015, respectively. Vehicle speeds have small influence on the prediction accuracy, and CA mortar disengagement degrees can be estimated well at both speeds. Therefore, the CDMEA shows good estimation robustness for various vehicle speeds.

5.2. Influence of Track Irregularities. In order to verify CMDEA under different track irregularities, the German low-disturbance spectrum was adopted and input into the algorithm, with the corresponding results shown in Figure 9.

It can be seen from Figure 9 that under the condition, the CA mortar disengagement degrees can also be estimated well except for limited incorrect estimates. The error E is 0.0048.

Track irregularities with larger amplitude have a great effect on the dynamic response than CA mortar disengagement, resulting in relatively large error values. Due to the larger amplitude of the German low-disturbance spectrum in the time domain compared with the China ballastless track spectrum, the estimation accuracy will be lower.

5.3. Influence of Noise. When assessing the effectiveness of CMDEA, its robustness with respect to measurement noise should be considered. To verify the tolerance to noise, the simulations were carried out by adding increasing Gaussian signal noise levels of 1%, 3%, 5%, and 10% (SNR 40 dB, 30.5 dB, 26 dB, and 20 dB) to the wheel acceleration signal before initiating CMDEA. The estimated and actual values of CA mortar disengagement degrees for this range of added signal noise levels are shown in Figure 10.

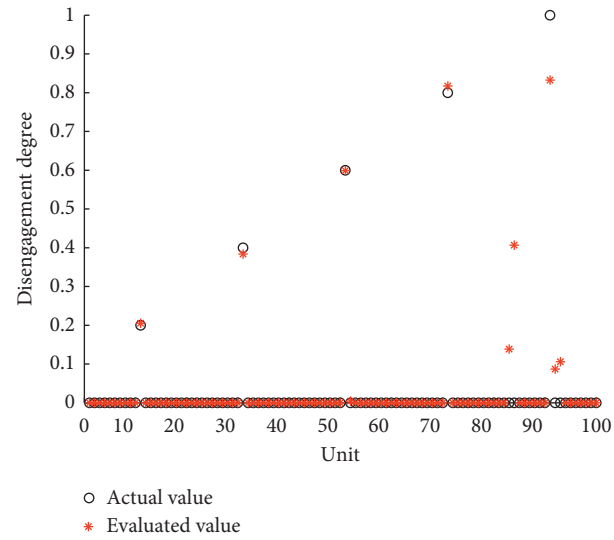

Figure 9: Estimation result of CMDEA with German low-disturbance spectrum.

It can be seen from Figure 10 that CA mortar disengagement degrees can be estimated under a lower level noise and even with a measurement signal noise of 10%. The estimation error is 9.9154e-04, 0.0012, 0.0015, and 0.0025. An increase in the level of signal noise results in an increase in the error of the estimated CA mortar disengagement degrees.

6. Conclusions

CA mortar disengagement of a ballastless track will induce changes of the dynamic response of a passing vehicle, which can accordingly be used to estimate the disengagement degree. In this paper, a novel method for estimating CA mortar disengagement degrees was described through an

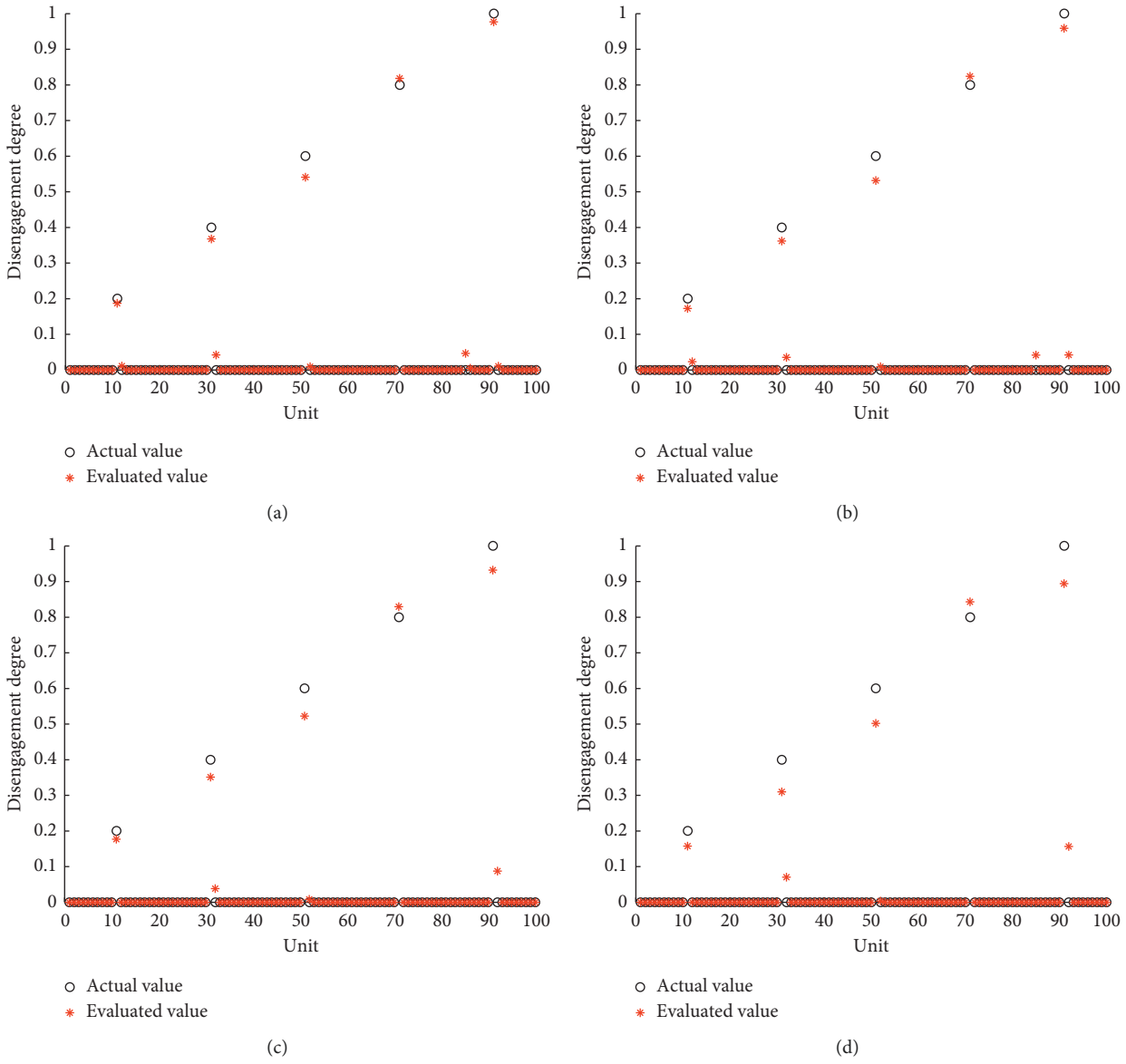

Figure 10: Estimation results of CMDEA under different noise levels: (a) 1% signal noise; (b) 3% signal noise; (c) 5% signal noise; (d) 10% signal noise.

analysis of wheel acceleration of a passing vehicle. The CMDEA employs an adapted genetic algorithm with a shifting window for parameter optimization, the process of which is split into a number of phases, and the initial value is given in terms of a prior probability. The CMDEA steps through the track in phases and obtains the overall disengagement degrees. The accuracy and robustness of the estimation were discussed.

From the simulation results presented in this paper, it is concluded that the CA mortar disengagement degrees estimated by the proposed algorithm are consistent with the hypothetical values assumed, and the robustness of the algorithm is validated under different track speeds, track irregularities, and signal noise levels. Compared with regular genetic algorithm, the improved algorithm has the advantages of a lower error value and much shorter total computation time. The CMDEA method in this paper assumes a convergence limit of 100. The effect of this upper limit value has not been investigated in this paper. Increasing the value will improve the accuracy of the method, but at a cost in computation time.

The proposed algorithm uses a vehicle-track coupling model and takes the simulated responses as field measurements to estimate CA mortar disengagement degrees. The theoretical analysis and simulation experiments have been carried out to obtain corresponding results and provide a theoretical basis for the field detection of CA mortar disengagement in the future. In the actual application process, due to the difference between the actual vehicle parameters and theoretical parameters, the estimation value of the actual CA mortar disengagement degree and the simulation result may be different. Therefore, future

experiments for the CMDEA involving the installation of measurement sensors are necessary to validate and improve the accuracy of CMDEA. Improving the robustness of the CMDEA by combining the characteristics of different line structures, vehicle types, and operating conditions is also an important direction for future research.

Data Availability

All data generated or analysed during the study are included in this paper.

Conflicts of Interest

The authors declare that they have no conflicts of interest.

Acknowledgments

This work was supported by the National Key Research and Development Program of China under Grant no. 2016YFB1200401 and the Technology Research and Development Program of China Railway under Grant no. 2017G002-A.

References

[1] Z. W. Lu, *Railway Track of Passenger Dedicated Line*, China Railway Publishing House, Beijing, China, 2005.

[2] M. Chen, "study on elastic wave field detection method used in under line layered structure of high-speed railway," Master's thesis, Shanghai Jiaotong University, Shanghai, China, 2014.

[3] Z. P. Hu, "Identify the depth of honeycomb in ballastless track concrete structure based on impact-echo method," *Railway Standard Design*, vol. 60, no. 10, pp. 22–26, 2016.

[4] P. F. Zhong, A. L. Che, S. K. Feng et al., "Typical defects' analysis and nondestructive detection method for undertrack structures of high speed railways," *Journal of Vibration and Shock*, vol. 36, no. 11, pp. 154–160, 2017.

[5] X. Tian, W. Zhao, Y. Du, and B. Wang, "Detection of mortar defects in ballastless tracks of high-speed railway using transient elastic wave method," *Journal of Civil Structural Health Monitoring*, vol. 8, no. 1, pp. 151–160, 2017.

[6] Z. F. Li, W. B. Xie, and T. Liu, "A detection method of CA mortar disengagement based on GBRT algorithm," *Journal of Railway Science and Engineering*, vol. 15, no. 2, pp. 292–301, 2018.

[7] A. Malekjafarian, P. J. McGetrick, and E. J. OBrien, "A review of indirect bridge monitoring using passing vehicles," *Shock and vibration*, vol. 2015, Article ID 286139, 16 pages, 2015.

[8] Y. B. Yang, C. W. Lin, and J. D. Yau, "Extracting bridge frequencies from the dynamic response of a passing vehicle," *Journal of Sound and Vibration*, vol. 272, no. 3–5, pp. 471–493, 2004.

[9] C. W. Lin and Y. B. Yang, "Use of a passing vehicle to scan the fundamental bridge frequencies: an experimental verification," *Engineering Structures*, vol. 27, no. 13, pp. 1865–1878, 2005.

[10] Y. Zhang, L. Wang, and Z. Xiang, "Damage detection by mode shape squares extracted from a passing vehicle," *Journal of Sound and Vibration*, vol. 331, no. 2, pp. 291–307, 2012.

[11] M. Molodova, Z. Li, and R. Dollevoet, "Axle box acceleration: measurement and simulation for detection of short track defects," *Wear*, vol. 271, no. 1-2, pp. 349–356, 2011.

[12] Z. H. Li and F. T. K. Au, "Damage detection of a continuous bridge from response of a moving vehicle," *Shock and Vibration*, vol. 2014, Article ID 146802, 7 pages, 2014.

[13] P. Quirke, D. Cantero, E. J. Obrien, and C. Bowe, "Drive-by detection of railway track stiffness variation using in-service vehicles," *Proceedings of the Institution of Mechanical Engineers Part F: Journal of Rail and Rapid Transit*, vol. 231, no. 4, pp. 498–514, 2017.

[14] W. M. Li, Z. H. Jiang, T. L. Wang, and H. P. Zhu, "Optimization method based on generalized pattern search algorithm to identify bridge parameters indirectly by a passing vehicle," *Journal of Sound and Vibration*, vol. 333, no. 2, pp. 364–380, 2014.

[15] J. Marzbanrad, P. Poozesh, and M. Damroodi, "Improving vehicle ride comfort using an active and semi-active controller in a half-car model," *Journal of Vibration and Control*, vol. 19, no. 9, pp. 1357–1377, 2012.

[16] M. A. Wardeh and H. A. Toutanji, "Parameter estimation of an anisotropic damage model for concrete using genetic algorithms," *International Journal of Damage Mechanics*, vol. 26, no. 6, pp. 801–825, 2015.

[17] S. Acikbas and M. T. Soylemez, "Coasting point optimisation for mass rail transit lines using artificial neural networks and genetic algorithms," *IET Electric Power Applications*, vol. 2, no. 3, pp. 172–182, 2008.

[18] Y. He and J. Mcphee, "Design optimization of rail vehicles with passive and active suspensions: a combined approach using genetic algorithms and multibody dynamics," *Vehicle System Dynamics*, vol. 37, no. 1, pp. 397–408, 2002.

[19] W. M. Zhai, *Vehicle-Track Coupling Dynamics*, Science Press, Beijing, China, 3rd edition, 2007.

[20] P. G. Li, X. Y. Liu, and G. Q. Li, "Influence of CA mortar void on dynamic characteristics of unit slab track on bridge," *China Railway Science*, vol. 35, no. 3, pp. 20–27, 2014.

[21] H. Shi, Z. J. Yu, and H. M. Shi, "An improved method for dynamic modelling of a slab track on a high-speed railway," in *Proceedings of the 15th International Conference on Railway Engineering Design and Operation*, pp. 225–237, WIT Press, Madrid, Spain, July 2016.

[22] H. Shi, Z. J. Yu, H. M. Shi, and L. Zhu, "Recognition algorithm for the disengagement of cement asphalt mortar based on dynamic responses of vehicles," *Proceedings of the Institution of Mechanical Engineers, Part F: Journal of Rail and Rapid Transit*, article 0954409718794018, 2018.

[23] P. Wang, H. Xu, and R. Chen, "Effect of cement asphalt mortar debonding on dynamic properties of CRTS II slab ballastless track," *Advances in Materials Science and Engineering*, vol. 2014, Article ID 193128, 8 pages, 2014.